Emulsion Polymerization of Voided Particles by Encapsulation of a Nonsolvent

Charles J. McDonald,* Kevin. J. Bouck, and A. Bruce Chaput

The Dow Chemical Company, Midland, Michigan 48674

Carl J. Stevens

UOP, Des Plains, Illinois 60016

Received August 2, 1999; Revised Manuscript Received January 10, 2000

ABSTRACT: The modification of an emulsion polymerization with a water-miscible alcohol and a hydrocarbon nonsolvent for the polymer can influence the morphology of the particles. The formation of monodispersed particles with a hollow structure or diffuse microvoids is possible. Both kinetic and thermodynamic aspects of the polymerization dictate which particle morphology is obtained. Complete encapsulation of the hydrocarbon occurs provided low molecular weight polymer is formed initially in the process. Subsequent addition of a cross-linking monomer stabilizes the morphology. The final particle size can be defined by small nucleating latex seed particles. Monodispersed hollow particles with diameters from 0.2 to 1 μm are possible. Void fractions as high as 50% are feasible. The phase separation of polystyrene within the styrene−isooctane dispersion has been modeled with the Flory−Huggins theory. The encapsulation has been discussed in terms of interaction parameters, transport processes, polymer molecular weight, and interfacial tension effects.

Introduction

The control of the morphology of latex particles has been an intensive area of research in emulsion polymer science for greater than 20 years. Technology has advanced such that a variety of structured particles are possible including core−shell, microdomain, and interpenetrating networks. These advances have been based on a deepening understanding of the thermodynamic and kinetic aspects of emulsion polymerization as well as more sophisticated approaches to processing. This ability to control particle morphology has enhanced significantly the range of physical properties accessible in application areas such as water-borne coatings.

Synthetic methods leading to particles having voids have also been extensively investigated. Hollow latex particles can serve as synthetic pigments, which contribute to the opacity of architectural coatings by scattering light.[1,2] In addition, these particles can enhance the gloss of paper coatings by influencing the mechanical properties of these high pigment volume concentration formulations during the calendering of the coating.[3,4] One of the earliest processes for making hollow latex particles was developed in the research laboratories of The Rohm and Haas Company.[5−10] Their concept involved making a structured particle with a carboxylated core polymer and one or more outer shells. The ionization of the carboxylated core with base under the appropriate temperature conditions expands the core by osmotic swelling to produce hollow particles with water and polyelectrolyte in the interior. In addition to this approach, a number of alternative processes have also been patented that are complex in terms of process stages and chemistry.[11−14]

In this paper, we describe an emulsion polymerization that involves an encapsulation of a nonsolvent hydrocarbon for the polymer being formed.[15] By encapsulation, it is possible to make latex particles having voids with facile control of particle diameter, void fraction, and structure. The process initially involves polymerizing a low molecular weight polymer that phase separates in a dispersed hydrocarbon−monomer mixture. This phase-separated polymer subsequently serves as a locus for polymerization of a cross-linked network that stabilizes the morphology. No high shear dispersion methodology is required to establish particle diameter, which can be defined by surfactant level or a nucleating latex seed concentration. By controlling the monomer conversion profile, monodispersed particles with structures ranging from microdomain to hollow are possible. This is illustrated with the particles shown in the transmission electron micrographs of Figure 1. Typically, the encapsulated hydrocarbon is removed by vacuum or steam stripping of the latex after completion of the polymerization. With sufficient network structure, the morphology is maintained in this process step.

Experimental Section

Materials. The raw materials required for the preparation of the latexes were used as supplied from the manufacturers. The monomers, styrene and divinylbenzene, were obtained from The Dow Chemical Company (Midland, MI) as were the surfactants, Dowfax 2A1and 8393. The divinylbenzene was a technical grade material containing 80 wt % of the divinyl monomer with the remaining 20 wt % being styrene and ethylstyrene. Methacrylic and acrylic acid were purchased from Rohm & Haas Company (Philadelphia, PA). The isooctane (Soltrol 10), *tert*-dodecyl mercaptan, dipentene dimercaptan, and ethylcyclohexyl dimercaptan came from Phillips Chemical Company (Bartlesville, OK). Methanol was purchased from Ashland Chemical Company (Columbus, OH). Sodium and ammonium persulfate were obtained from Fisher Scientific (Pittsburgh, PA). Rhodacal DS-10 was obtained from Rhone Poulenc (Cranbury, NJ).

Latex Synthesis. The latexes were prepared in a jacketed, pressurized, computer-controlled 1 gal stainless steel reactor equipped with a mechanical stirrer and inlet tubes for the continuously added monomer and initiator feeds. The temperature was controlled to within ±1 °C with steam and water in the jacket. The initial charge and the monomer feeds were blanketed with nitrogen during the polymerization.

10.1021/ma991284e CCC: $19.00
Published on Web 02/16/2000

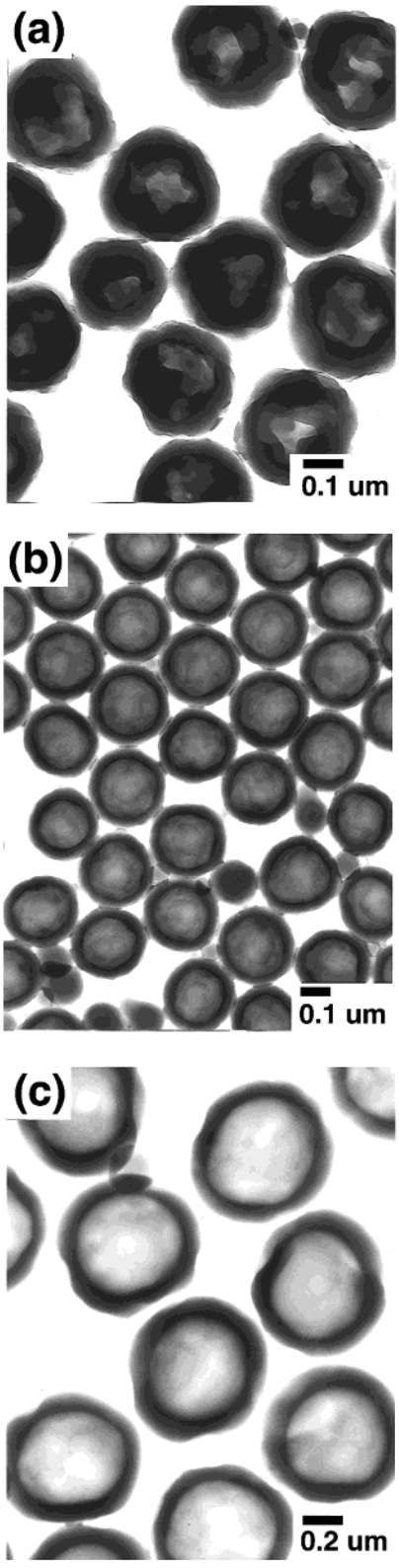

Figure 1. Transmission electron micrographs of (a) microvoided latex particle, (b) hollow latex particle with 30% void volume, and (c) hollow latex particle with 50% void volume.

Seed Latex Synthesis. The encapsulation stage in this process can be carried out under both seeded and nonseeded conditions. The influence of seed size and molecular weight on encapsulation will be discussed in a later section. The seeds examined in this study ranged from 0.0280 to 0.3200 μm, and their molecular weights were adjusted by adding various amounts of the chain transfer agent, *tert*-dodecyl mercaptan [TDDM], to the process. The seeds, copolymers of styrene with small amounts of acrylic acid, were prepared in a semicontinuous process in a jacketed reactor similar to that described above. An example recipe is given in Table 1. In this case, 1.0 part of TDDM was incorporated in the initial charge, and the weight-average molecular weight was 52 400 as measured by GPC.

Table 1. Recipe and Polymerization Parameters

steam	component	parts[a]
A	water	366.05
	Rhodacal DS-10	0.12
B[b]	styrene	98.50
	water	33.23
	acrylic acid	1.50
	Rhodacal DS-10	0.05
C	*tert*-dodecyl mercaptan	1.00
D	water	0.875
	ammonium persulfate	0.370

stream	feed fraction	start time (min)	end time (min)
B	0.05	0	3
D	1.0	3	5
C	1.0	20	20
B	0.95	20	85

parameter	value
target particle size	3000 Å
charged solids	20.2%
polymerization temp[c]	85 °C
hold time[d]	15 min

[a] Based on 100 parts monomer. [b] Stream was emulsified by shaking. [c] Initial temperature was 78 °C for 15 min. [d] Time for which the reactor is kept at temperature following the end of monomer feeds.

Latex Characterization. The particle size of the latexes at various stages of the process were characterized via hydrodynamic chromatography.[16,17] The percent solids of the latexes were determined by drying 1−2 g of latex at 140 °C in a vented oven for 30 min.

Gel Permeation Chromatography Analysis. The molecular weight distributions of the seeds and the initial stage polymers were characterized by gel permeation chromatography [GPC]. The samples were prepared by placing 20 mg of material in 10 mL of tetrahydrofuran and passing the solution through a 0.2 μm filter. If an observable gel fraction was present, it will be noted with the data. The chromatograph consisted of a Waters M-6000 pump (1.0 mL/min), a Waters WISP 710B injector with 75 μL injection loop, two Polymer Labs 5 μm Mixed-C batch columns (at ambient temperature), and a Waters 410 DRI refractive index detector (at 35 °C). The software used to collect and analyze the data was Polymer Laboratories' Calibre GPC/SEC Version 6. The instrument was calibrated using narrowly distributed polystyrene molecular weight standards obtained from Polymer Laboratories. The eluent was HPLC grade tetrahydrofuran, purchased from Fisher Scientific (Pittsburgh, PA), was unstabilized and sparged with helium.

Results and Discussion

Process Characterization. The schematic in Figure 2 can serve as a starting point to describe in detail this process for making voided latex particles. It is broken down into two stages: an initial encapsulation stage followed by a stabilization stage. This particular schematic and the majority of the data that follows address the development of a hollow particle. An example of a polymerization recipe is shown in Table 2.

The first stage involves polymerizing a batch monomer charge containing a small amount of vinyl carboxylic acid. Also present in the batch charge are a surfac-

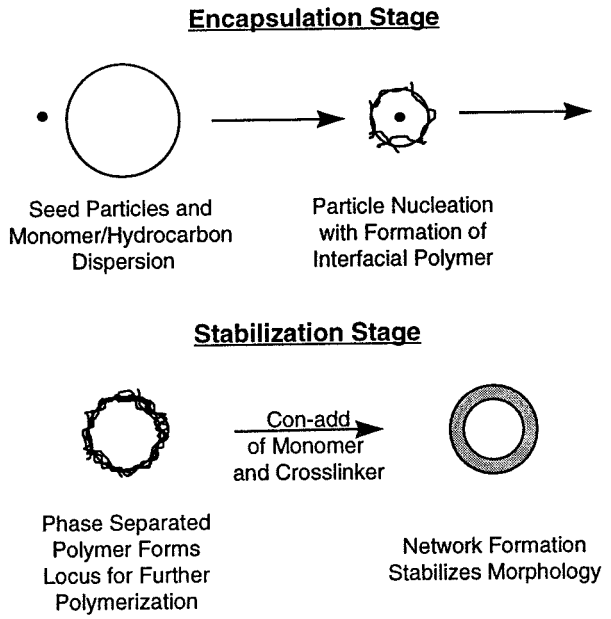

Figure 2. Schematic of two-stage voided latex particle process.

Table 2. Recipe and Polymerization Parameters for Hollow Latex Particles

steam	component	parts[a]
A	water	130.41
	isooctane	35.50
	styrene	28.02
	methanol	20.25
	methacrylic acid	1.00
	dipentene dimercaptan	0.61
	seed latex	0.03
B	water	22.06
	sodium persulfate	1.10
C	water	19.10
	DOWFAX 8390	0.57
	DOWFAX 2A1	0.50
D	styrene	60.47
	divinylbenzene 80	10.00
	methacrylic acid	0.50

stream	feed fraction	start time (min)	end time (min)
B	0.5	0	75
B	0.5	75	300
C	1.0	75	270
D	1.0	75	300

parameter	value
target particle size	4200 Å
charged solids	31%
polymerization temp[c]	90 °C
hold time[d]	30 min

[a] Based on 100 parts monomer. [b] Time for which the reactor is kept at temperture following the end of monomer feeds.

tant, a chain transfer agent, a water-miscible alcohol, and a hydrocarbon. In our study, styrene, methacrylic acid, methanol, and isooctane were used. Typically, the molecular weight of the polymer formed in this stage of the process is below 50 000. The isooctane is a nonsolvent for the polystyrene, and as monomer is consumed, the polymer becomes progressively less compatible with the dispersed hydrocarbon/monomer mixture. Phase separation of the polymer is observed to occur primarily at the interface of the particle. It is believed that this surface concentration is preferentially formed because the water−polymer interface has the lowest interfacial energy in the system. In addition, the water-soluble thermal initiator generates aqueous phase radicals, including oligomeric radicals, which are adsorbed and anchored to the surface of the dispersion. The surface appears to become the primary site for polymerization with the monomer concentration being replenished by diffusion through both the serum phase of the emulsion and the encapsulated internal hydrocarbon mixture. This surface polymer also serves as the polymerization locus for the continuously added monomer charge introduced during the second, or stabilization, stage of the process. Included in this second charge is a cross-linking monomer, which forms a network polymer. With styrene-based copolymers, divinylbenzene was the cross-linking monomer.

The electron micrographs shown in Figure 3 are of samples taken during the course of this two-stage process. Figure 3A is a micrograph of the initial charge shortly after the start of the polymerization. This polymerization was seeded with small (0.028 μm) polystyrene particles added to the initial charge to serve as nucleation sites for particle growth. Particle size control is possible with this process with or without the use of seed particles.

As the polymerization proceeds, a polymeric gel at the surface of the particles become visible (Figure 3B). Subsequently, the size distribution of the particles is seen to narrow; that is, the colloid is digested. This is shown in Figure 3C. Thus, monomer and hydrocarbon equilibrate through the water phase to the nucleated sites at this point in the process.

Figure 3D is an electron micrograph of the second stage of the process when the cross-linking monomer stream is continuously added. The start time of addition of the second monomer charge is crucial to defining the ultimate morphology of the particle. If the monomer conversion of the batch charge exceeds approximately 20−40% instantaneous conversion, the phase-separated polymer fills the entire particle leading to a microdomain structure. The exact instantaneous monomer conversion required for hollow morphology is dependent on the amount of hydrocarbon present. With either morphology, the end result is a particle with a stable morphology with a fully encapsulated charge of hydrocarbon.

This particular polymerization had the objective of making a 0.4200 μm particle with a 33% void fraction. However, a range of particle diameters and void fractions are possible. The largest particle made in this study had a diameter of 1 μm with a 50% void fraction. The smallest had a diameter of 0.2300 μm with a 33% void fraction. The electron micrographs in Figure 3 are of samples that have aged for about 1 week after they were removed from the reactor. There was no phase separation of the hydrocarbon during this period; hence, the morphologies pictured are thermodynamically stable. Further, a radical scavenger was added to these samples after removal from the reactor to prevent further polymerization.[18]

In addition to microscopy, the process can be characterized in terms of conversion kinetics and particle diameters. These data for the polymerization recipe in Table 2 are given in Table 3. This recipe again is for a 0.4200 μm hollow particle with a 33% volume fraction of hydrocarbon. In this data set, the continuously added monomer charge was started at 75 min, at approximately 30% conversion of the initial charge. The particle

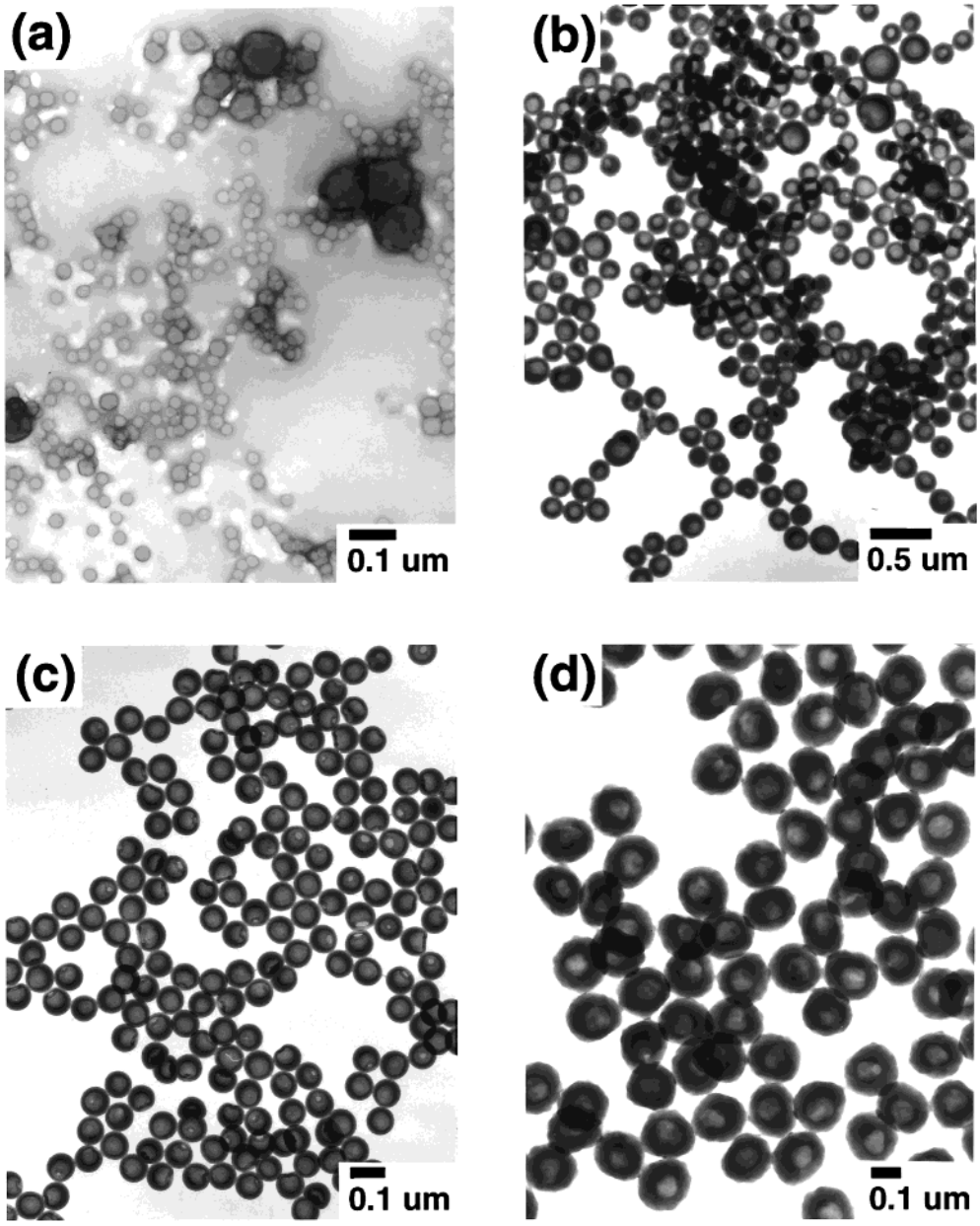

Figure 3. Transmission electron micrographs of samples removed during seeded encapsulation process: (a) early encapsulation stage, (b) intermediate encapsulation stage, (c) end of encapsulation stage, and (d) intermediate stabilization stage.

Table 3. Instantaneous Percent Monomer Conversion and Particle Size as a Function of Polymerization Time

polymerization time (min)	instantaneous % conversion	particle size (μm)
75	31.6	0.1800
150	58.3	0.3000
225	91.2	0.3700
300	92.2	0.4000
final	99.9	0.4100

sizes were measured with hydrodynamic chromatography (HDC) which is believed to underestimate the actual diameter because the monomer component in the hydrocarbon mixture has an affinity for the column packing material, polystyrene beads.

A sense of the solution conditions in the hydrocarbon mixture under which the initial stage low molecular weight polymer phase separates can be obtained with the data in Table 3. At 75 min, the amount of polymer formed in the emulsion is 4 wt % or in terms of instantaneous conversion 30%. This is sufficient to establish the surface polymer layer. Considering only the dispersed particles themselves, this corresponds to a polymer solution concentration in the hydrocarbon mixture of approximately 13 wt %, assuming a uniform distribution throughout the particle, or 34 wt % if all of the polymer is concentrated in an outer shell of 0.0300 μm thick. Another assumption involved with these calculations is that the hydrocarbon mixture is completely associated with the particle; i.e., no reservoir exists in the dispersion. At this point of the polymerization, the composition of the mixture has decreased from 45 wt % monomer to approximately 36 wt %.

During the addition of the second monomer charge, the conversion kinetics could be adjusted by variation of the rates at which the monomer and the initiator streams are fed. It was found that uniform conversion kinetics during both stages of the process is ideal in terms of encapsulation and morphology. Accelerating the kinetics during the stabilization stage can reverse the extent of encapsulation, while slowing the kinetics

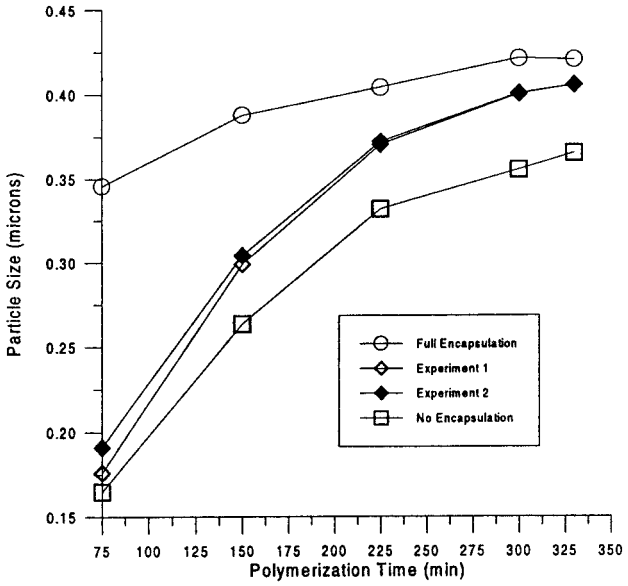

Figure 4. Calculated particle size with and without encapsulation compared with experimental data.

would lead to swelling of the particles and a thickening of the shell polymer.

The experimental particle diameter growth data can be compared with calculated estimates based on simple geometric equations knowing the number of seeds and the densities of the components. Four curves are displayed in Figure 4. Two represent replicates of the HDC experimental data mentioned above. The other two are calculated. The curve identified as "full encapsulation" assumes that the monomer and hydrocarbon are completely associated with the seed; i.e., no monomer−hydrocarbon reservoirs exist in the emulsion. The curve labeled "no encapsulation" assumes that only polymer is associated with the seed; i.e., instantaneous conversion is very high. The experimental curves are situated intermediate between the two calculated curves except during the latter third of the process where it approaches the full encapsulation curve. These data suggest that a monomer−hydrocarbon reservoir exists throughout the first two-thirds of the process even though a shell polymer is in place. Thus, diffusion of both nonsolvent hydrocarbon and monomer into the particle appears to be possible beyond the encapsulation stage. This is reinforced by the electron microscopic data, shown previously, illustrating that the particle size distribution narrows during this intermediate stage of the process. The HDC data in Figure 4 can, however, be compromised by the following factors: extraction of styrene monomer into the column packing, the fragility of the particles to shear forces in the HDC column, and the detection software which depends on UV adsorption to calculate the particle size distribution.[17] Independent of this, the reproducibility of these data is very good as also shown in Figure 4.

The above data indicate that this process is complicated, influenced by a number of convoluted thermodynamic and kinetic factors. It could be described as a dispersed solution polymerization in a mixed solvent system, the good solvent component being monomer. As monomer is consumed, the polymer phase separates and fills the particle from the surface inward. The ultimate morphology is defined by the extent the phase separation is allowed to proceed. This is controlled in the process by the start time of the continuously added monomer charge that forms a network copolymer. This process is also complicated by some nontraditional aqueous phase serum chemistry for an emulsion polymerization due to the presence of the alcohol. Though the thermodynamic and kinetic aspects of this process are convoluted, experimental variables could be adjusted to gain control over morphology, monodispersity, the extent of encapsulation, and the amount of coagulation. These will be described below.

Variables. (a) Initial Stage Polymer Molecular Weight. It has been observed that low molecular weight polymer must be made initially in order to encapsulate the hydrocarbon mixture. If the polymer has a molecular weight greater than 100 000, the hydrocarbon tends to concentrate as a layer on the top surface of the emulsion. The particle diameter growth curve for the polymerization where none of the isooctane is encapsulated is included in Figure 4.

The molecular weight of the initial stage polymer is influenced by the amount of chain transfer agent (CTA), the initiator concentration, and the amount of alcohol present. The most efficient variable to control molecular weight was the CTA level and type. Encapsulation has been found to be maximized with a molecular weight below 50 000. For the recipe in Table 2, the molecular weight was typically around 8000.

The initial stage polymer later becomes the locus of a network polymerization. During this transition, polymerization occurs in the presence of the CTA as well as cross-linking monomer. Controlling the growth in molecular weight is important to optimize encapsulation and the shell thickness of the hollow particle. Various CTAs were examined in terms of their efficiency and longevity. The molecular weight of the initial stage polymer was obtained with gel permeation chromatography (GPC) over an extended period of time. The goal was to define conditions under which polymer of continuously increasing molecular weight was formed and to minimize the influence of the CTA in the second stage of the process. The CTAs examined consisted of mercaptans and dimercaptans. They included *tert*-dodecyl mercaptan (TDDM, **1)**, ethylcyclohexyl dimercaptan (ECDM, **2),** and dipentene dimercaptan (DPDM, **3)**. Each were studied at equal molar concentrations. It could be expected that, as the second active hydrogen of the mercaptan undergoes reaction, the average molecular weight of the polymer would increase.

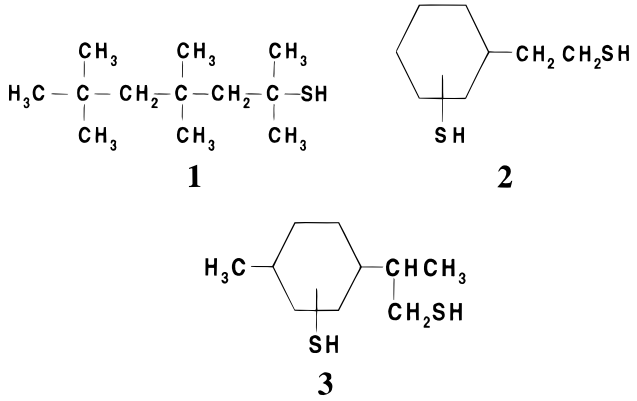

Figure 5 contains a series of GPC traces characterizing the influence of these three mercaptans on the molecular weight of the initial stage polymer as a function of time. Figure 5a describes the molecular

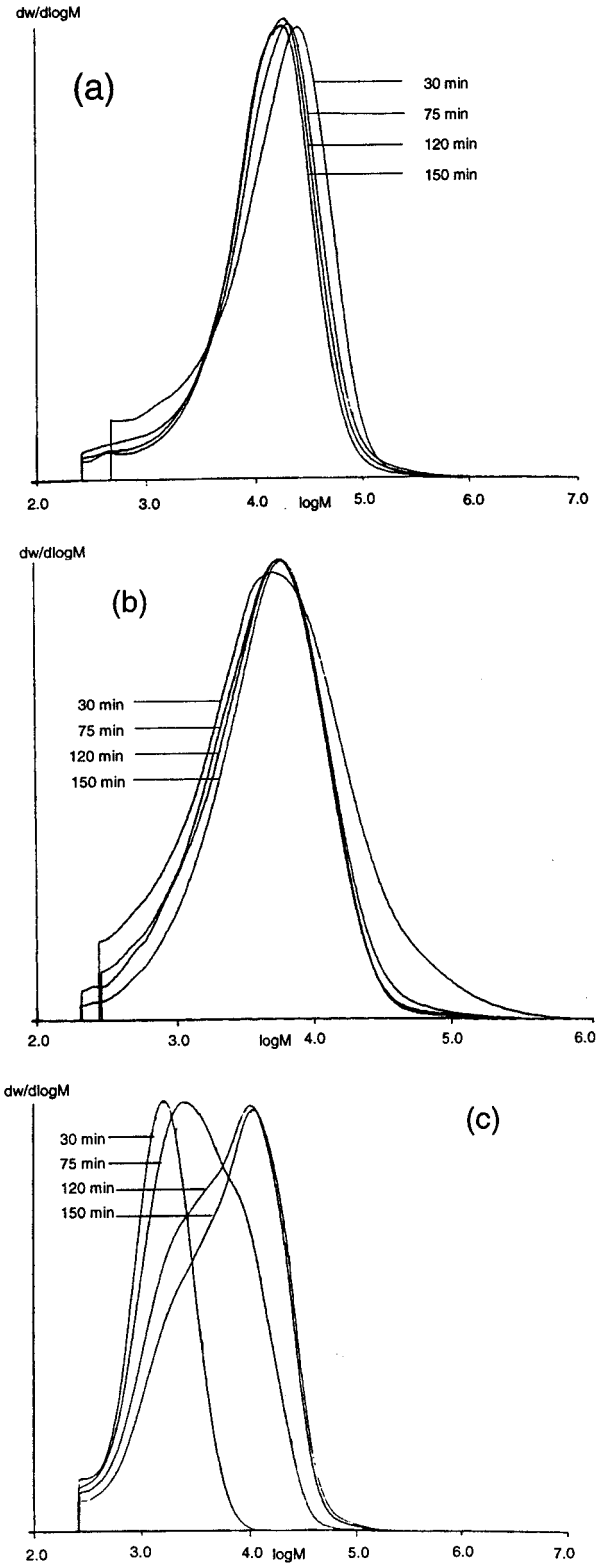

Figure 5. Overlaid GPC samples of polymer from batch stage with (a) no CTA, (b) with TDDM, and with (c) DPDM.

weight variation over 2.5 h without any CTA present. Figure 5b indicates the influence of TDDM in the same monomer mixture over the same time period. Figure 5c is identical data except that the dimercaptan, DPDM, is present. In addition to the decrease in the molecular weight relative to the control, the dimercaptans give a unique time dependence to the molecular weight change. That is, the average molecular weight shifts to higher values as the initial stage polymerizes. This was interpreted as indicating that, after incorporation of the dimercaptan into a polymer chain, the second active hydrogen contributes to the development of molecular weight. This differs from the monomodal, uniform molecular weight generated with the TDDM system over time.

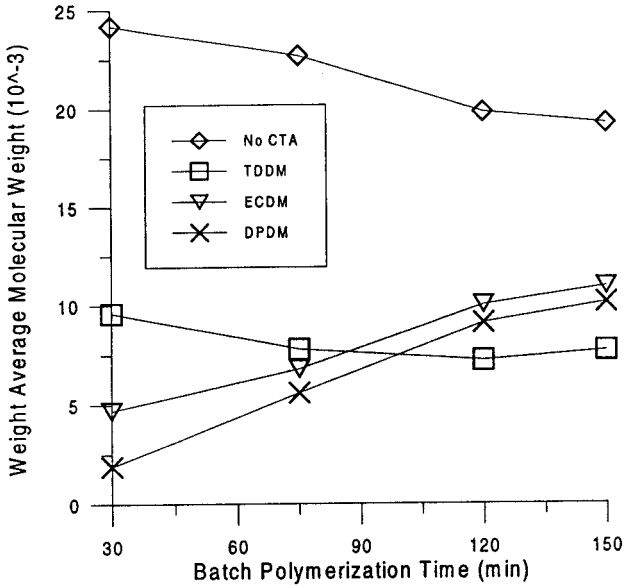

Figure 6. Weight-average molecular weight of batch polymer as a function of time and chain transfer type.

The weight-average molecular weight values are plotted as a function of time in Figure 6. The molecular weight decrease over time for the polymerization without mercaptan, as well as for that with the TDDM, is believed to be associated with the decrease in the amount of monomer present as the conversion increases. The molecular weight for the initial stage polymer made without any mercaptan is still quite small under these polymerization conditions. This is related to both alcohol being present, as will be discussed later, and the fact that the locus of polymerization is a diluted solution of monomer. It is also apparent in the figure that with the dimercaptans the initial molecular weight is the smallest and tends to increase over the course of the polymerization. This increase is most prominent with DPDM. The molecular weight transition facilitated with the dimercaptans proved most effective in ensuring that the hydrocarbon was fully encapsulated.

In addition to encapsulation, the regularity of the shell structure is influenced by the molecular weight. Figure 7 contains the electron micrographs of the particles near the end of the encapsulation stage formed in the presence of various amounts of TDDM. These electron micrographs are of samples all at 33 wt % instantaneous monomer conversion. The specific molecular weights are given in Table 4. These micrographs characterize the phase separation early in the process and introduce another critical variable for particle morphology, the shear in the reactor. It is apparent that as the TDDM increases and the molecular weight decreases, the particles become more irregular and distorted. Without the chain transfer agent, the particles have greater uniformity and have undergone the largest amount of phase separation (Figure 7a), approaching the microdomain morphology as the polymer spreads throughout the particle. All the data in Figure 7 were obtained under the same reactor agitation

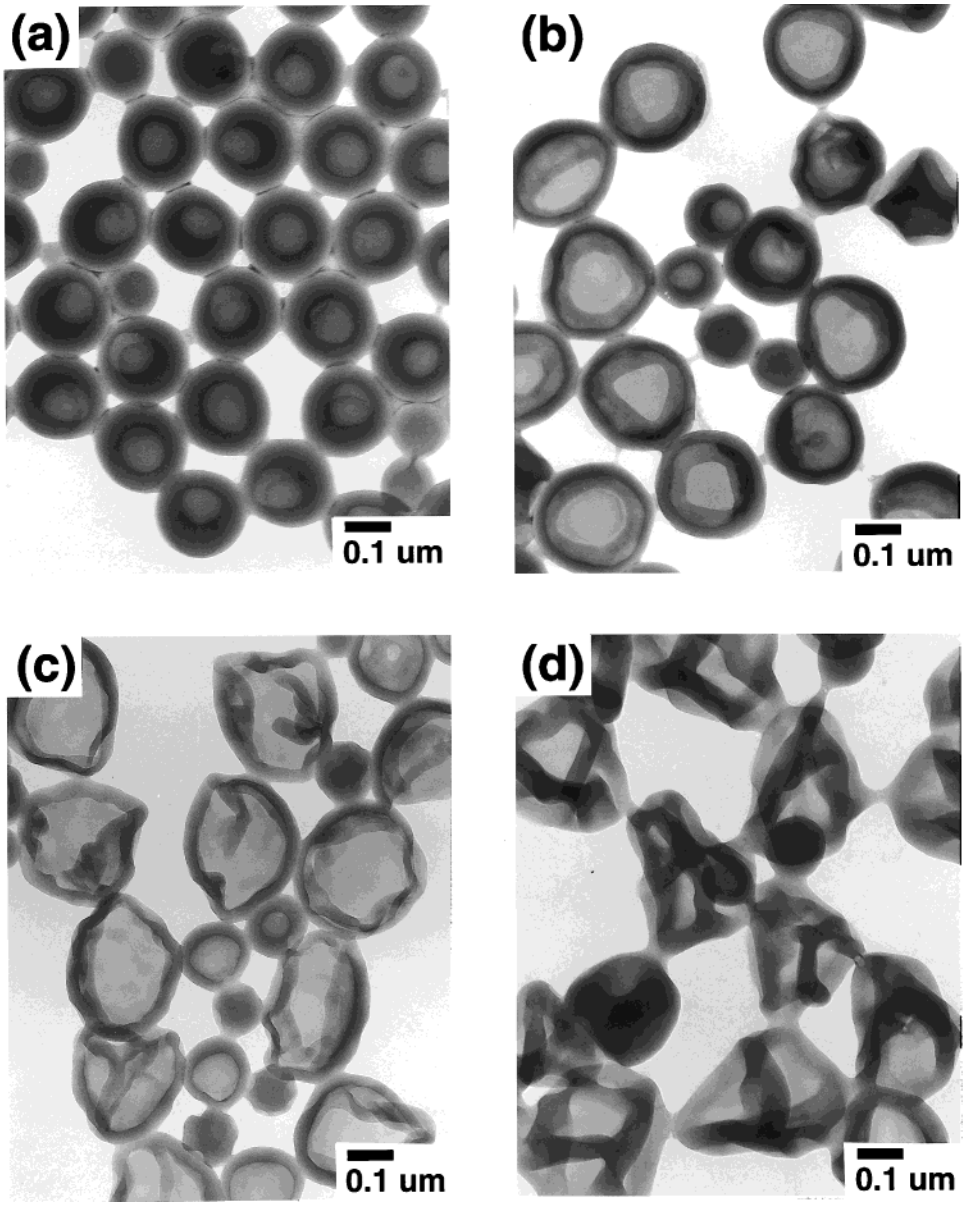

Figure 7. Transmission electron micrographs of encapsulation stage latex particles made with (a) no, (b) 0.3 part, (c) 0.6 part, and (d) 1.2 parts TDDM.

Table 4. Weight-Average Molecular Weight of Batch Polymer Made with Various Levels of TDDM

TDDM level (parts)	M_w
0	18000
0.6	5900
1.2	3400

conditions which were sufficient to mix the hydrocarbon throughout the continuous phase. This agitation was provided by a typical reactor stirrer: no high shear mechanical mixing equipment is required in this process. By balancing the shear within the reactor and the molecular weight, a range of polymerization conditions were defined that maximized the uniformity of a given morphology.

It was also possible to monitor the molecular weight growth over both stages of the process described in Table 1 by replacing the DVB with styrene. This ensured generation of linear polymer throughout which could be analyzed by GPC without any ambiguity. The molecular weight formed later in the process was observed to be significantly higher than the initial stage polymer. This is illustrated in the overlaid GPC curves in Figure 8. This is interpreted as due to the fact that the locus of polymerization changes as the polymerization proceeds.

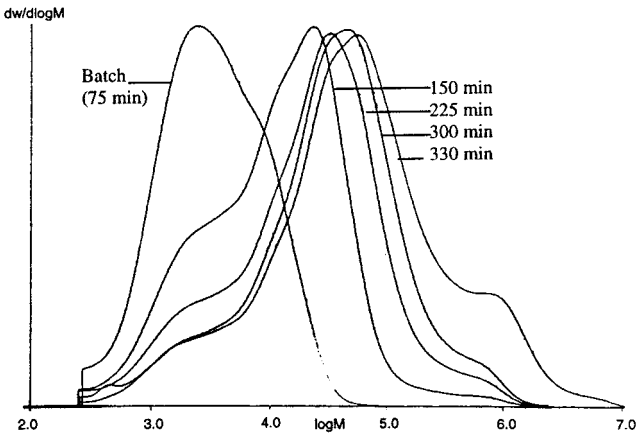

Figure 8. Overlaid GPC traces of polymer made during encapsulation process without any DVB.

Table 5. Weight-Average Molecular Weight of Batch Polymer Made in the Presence of Various Alcohols

alcohol	weight %[a]	M_w
none		323 000
methanol	16	183 000
methanol	32	125 000
2-propanol	16	133 000
ethanol	16	176 000

[a] Based on aqueous phase.

(b) Water-Miscible Alcohol. The water-miscible alcohol plays a crucial role in this process influencing molecular weight development, the solubility and transport properties of the serum phase of the emulsion, the interfacial tensions, and the polymerization kinetics.

The influence of alcohol level and type on the molecular weight of the initial stage polymer is shown in Table 5. These data are for the process run at 70 °C. (Note: the previous data were for the 90 °C process; Table 2.) By introducing an alcohol, the molecular weight decreased substantially with the effect becoming more pronounced as the level increases. On a relative basis, 2-propanol appears to be the most effective.

The actual causes for the molecular weight decrease, however, are ambiguous in that a number of phenomena occur when alcohol is introduced into the serum of this emulsion polymerization. For example, in the absence of alcohol, encapsulation is limited, and the polymerization is similar to a traditional emulsion polymerization with the hydrocarbon layered on the surface of the latex. The locus of polymerization is within the monomer-swollen particle instead of within the dispersed hydrocarbon−monomer−polymer mixture. The molecular weight is comparable to that expected from emulsion polymerization theory.[19] Thus, introducing alcohol changes the nature of the polymerization locus, diluting the monomer, creating solution like polymerization conditions.

Further, the alcohol can participate in a chain transfer reaction with the growing polymer chains[20] and an oxidation reaction with the thermal initiator, sodium persulfate.[21,22] The reaction with the thermal initiator involves the oxidation of the alcohol by a free-radical mechanism.[23] This is a competitive reaction for the persulfate radicals. In addition, the solubility and transport properties of the serum phase change significantly with the addition of alcohol. This would be expected to affect the adsorption and desorption of oligomeric radicals, a variable critical to the modeling of emulsion polymerization.[24] All the above interactions would change the nature of the polymerization, with the ultimate effect, observed through experiment, being a lowering of the molecular weight and a slowing of the conversion kinetics. The kinetic data will be discussed in more detail in the following section.

The efficiency of the encapsulation of the isooctane in the presence of alcohol is related to the lowering of the interfacial tensions in this emulsion system. This will become more apparent when discussing the equilibrium model for this process in a later section. The interfacial tensions, however, can be examined by experiment. The various surfaces in this process are illustrated in Figure 9. The system is comprised of three distinct phases. These include the relatively large droplets of the monomer−hydrocarbon mixture having an organic−aqueous interface (phase I) and two phases within the relatively small latex particles, a polymer-rich phase (phase II) as well as a hydrocarbon-rich phase (phase III). The quantitative relationships governing the effect of the interfacial tension on the chemical potentials in these three phases are also contained in the figure. They are described in terms of the activity of species, *i*, in which *i* may be styrene, isooctane, or polystyrene.

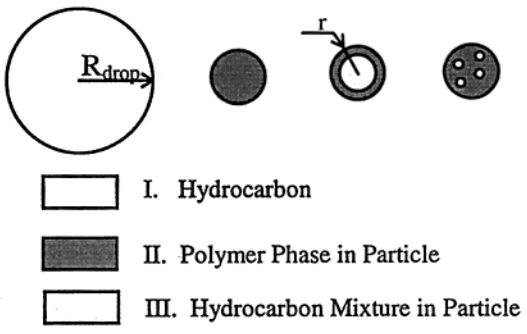

A] Hydrocarbon Mixture in Droplets.

$$a_i = a_{i^o} e^{\left(\frac{2\sigma_{I,water}V_i}{R_{drop}RT}\right)} \approx a_{i^o}$$

B] Polymer Phase in Particle.

$$a_i = a_{i^o} e^{\left(\frac{2\sigma_{II,water}V_i}{rRT}\right)}$$

C] Hydrocarbon Mixture in Particle.

$$a_i = a_{i^o} e^{\left(\frac{2\sigma_{II,water}V_i}{rRT}\right)} e^{\left(\frac{2\sigma_{II,III}V_i}{r_{core}RT}\right)} \approx a_{i^o} e^{\left(\frac{2\sigma_{II,water}V_i}{rRT}\right)}$$

Figure 9. Interfacial tension effect on activities of phases in process.

Because of the large diameter of the hydrocarbon−monomer droplet, the interfacial tension effect on its constituents can be ignored (eq A, Figure 9). For a latex particle without phase separation, the effect of interfacial tension is given by eq B. When phase separation is present, eq C is applicable. It indicates that the chemical potentials of the species in the core of the particle are modified by both the interfacial tension at the particle/aqueous interface and that between the two phases within the particle. The latter is considered to be small and will be ignored. This analysis illustrates that the equilibrium between the monomer−hydrocarbon droplet and the latex particle is influenced significantly by interfacial tension.

To estimate the magnitude of the effect of interfacial tension, it was thought important to examine the various surfaces in this process. Methanol is a constituent in the continuous phase of this emulsion polymerization. Over the course of the work, it was varied in a range of 10−30 wt % of the aqueous phase. The recipe in Table 2 indicates a level of approximately 10 wt % in the water. The influence of methanol on the aqueous−hydrocarbon interfacial tension was substantiated by experiment. This involved measurements of the interfacial tension of the aqueous−methanol interface against isooctane, ethylbenzene, and an 80/20 mixture of polystyrene and ethylbenzene. Ethylbenzene was used in

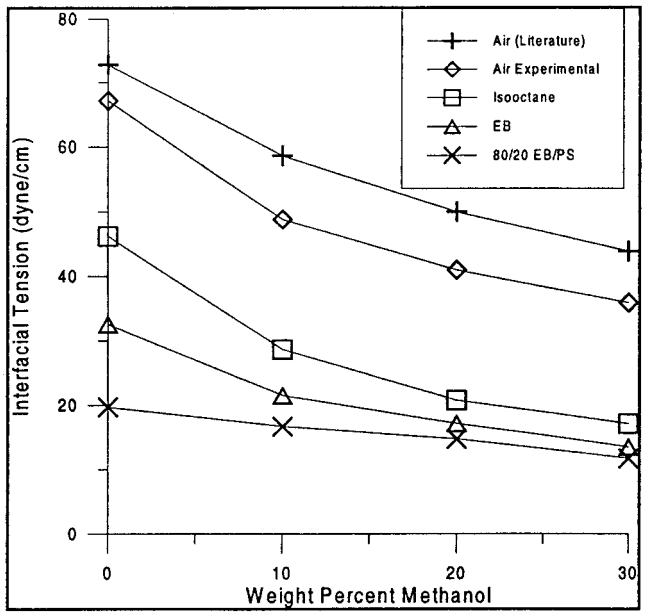

Figure 10. Interfacial tension values between various materials, or mixtures, and water−methanol solutions.

these experiments as a substitute for styrene, a more reactive and hazardous hydrocarbon. These data are plotted in Figure 10. Included for comparison are data for the air/aqueous methanol interface as compared to literature values.[25] Consistently, the interfacial tension decreases as methanol level increases up to a 10% level. Beyond that level, little effect is observed. Also, the rate of change is largest for the isooctane/aqueous methanol interface. Experimental data indicated that encapsulation was maximized in the presence of methanol, and the level present was minimized to approximately 10 wt % in the aqueous phase based on these data.

(c) Conversion Kinetics. During the course of this study, a variety of polymerization conditions were examined to optimize the morphology, reduce polymerization time, and minimize any coagulated polymer produced in the process. This involved variation in process variables such as temperature and feed rates as well as recipe components such as alcohol level and type, surfactant system, initiator concentration, and monomer composition. The process described in Table 1 was effective in making monodispersed hollow particles with complete encapsulation of the hydrocarbon with minimal waste. It will be the focus of our description of conversion kinetics.

In the transition from the encapsulation stage of this process to the stabilization stage, the conversion kinetics were intentionally kept constant. As mentioned, accelerating the kinetics during the stabilization stage diminished the amount of hydrocarbon that was encapsulated, while slowing the conversion led to swelling of the polymerization locus, thickening the polymer shell. The amount of coagulated latex also increased as the conversion rates slowed.

Independent of the change in polymerization loci from a hydrocarbon solution to a phase separated polymer, the conversion kinetics could be made uniform by varying the amount of persulfate introduced into the process over the stages of the polymerization (Table 2). One would expect the polymerization to accelerate when it occurs within the matrix of phase separated polymer relative to the initial solution conditions. By decreasing

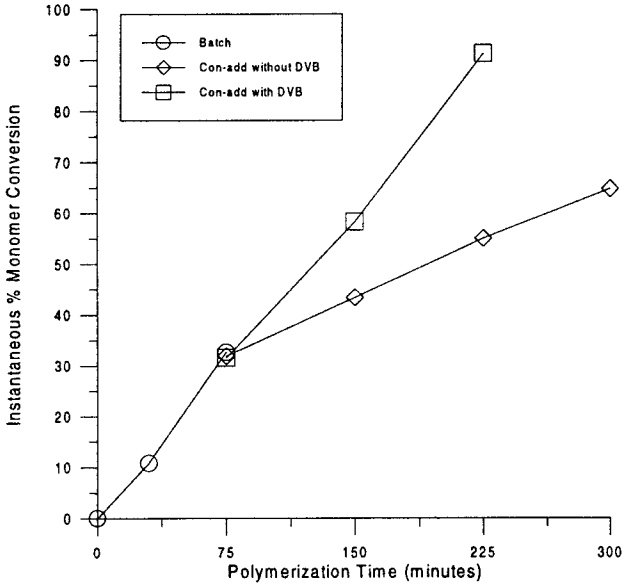

Figure 11. Instantaneous percent monomer conversion as a function of polymerization time conducted with and without the cross-linker DVB.

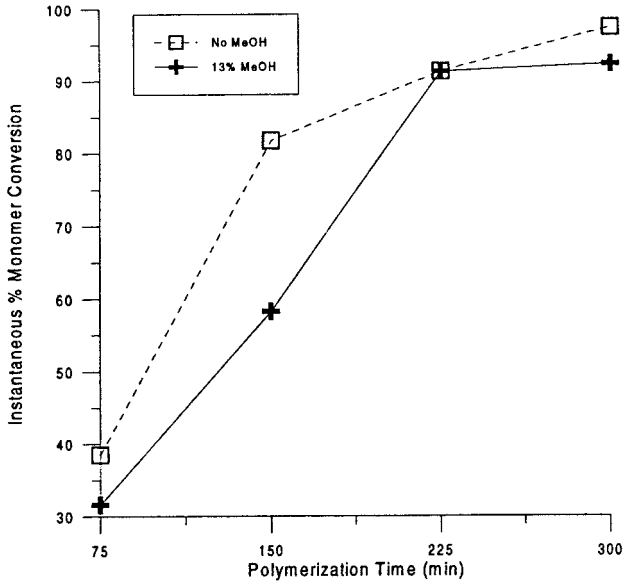

Figure 12. Instantaneous percent monomer conversion as a function of polymerization time conducted with and without methanol.

the rate at which persulfate was added during the latter stage of the encapsulation, the kinetics could be moderated. In Figure 11 the instantaneous percent monomer conversion versus time is plotted. This figure covers the conversion of both the encapsulation as well as for the stabilizing stages, the latter with and without DVB. There is little or no apparent difference in the rate of polymerization for these stages with DVB present. However, the rate of polymerization is lower for the DVB-free process due to the absence of the Trommsdorff effect.[26]

In the previous section, mention was made of the effect alcohol had on molecular weight, and reference was made to it also having a significant influence on polymerization kinetics. Quantitative data describing the kinetic effect are contained in Figure 12. It is apparent in Figure 12A that introducing methanol into the process decidedly slowed the conversion kinetics.

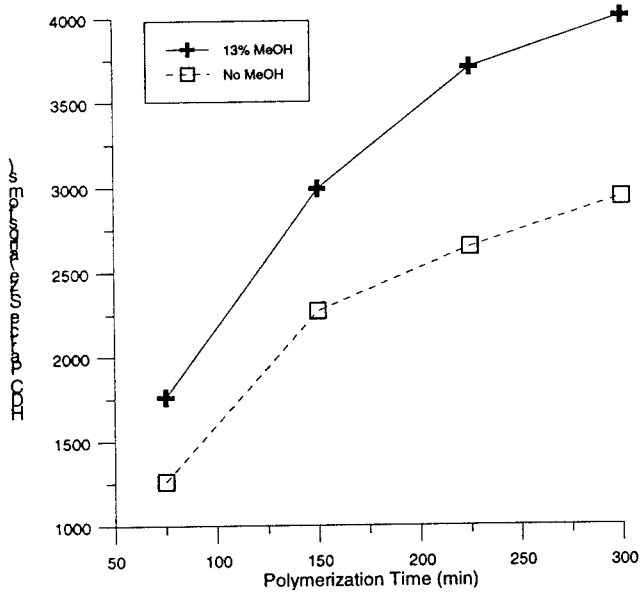

Figure 13. Latex particle size as a function of polymerization time conducted with and without methanol.

Figure 13 provides an explanation in that the particle size in the presence of alcohol is considerably larger that in its absence, again indicating the improved level of hydrocarbon encapsulation occurring with alcohol.

(d) Particle Size Control. In an emulsion polymerization, nucleation sites can be established by various mechanisms.[27] The easiest way to control particle size is through the use of seed particles that are introduced into the initial reactor charge. This seeded approach has other advantages, such as narrowing the particle size distribution and minimizing the use of surfactants or other stabilizing species. The latter can introduce foaming tendencies to a latex and water sensitivity to films made from these dispersions. When an emulsion polymerization is under seed control, the final particle size is identical to that determined by a simple geometric calculation involving the density of the polymer, the weight and diameter of the initial seed charged, and the volume of monomer incorporated into the particle. In a traditional emulsion polymerization, seed control exists over a particle size range for a given seed size. For example, attempting to make a very large particle, e.g., 1 μm, from a small seed, $\leq$0.1 μm, produces a secondary crop of smaller particles. This is caused by the surface area being decreased during particle growth, leading to desorbed surfactant stabilizing additional nucleation sites during the course of the polymerization.[28]

This encapsulation process exhibits seed control. The final particle size was identical to that calculated, as described above, with the hydrocarbon fraction included as a volume component. Figure 14 compares the final particle diameters obtained for a series of seed of increasing diameter. The dotted line was calculated on the basis of the seed controlling the final particle size. These seeds are characterized in terms of their diameters and molecular weights in Table 6. In this series, cross-linked polystyrene hollow particles were made with a 33% void fraction except for the 1 μm particle, which had a 50% void fraction. Seed control is exhibited over a finite size range depending on the particular seed. In this process loss of seed control is characterized by the experimental diameter being below that calculated. This was caused by the generation of a second population of smaller particles. Because of the dependence of the conversion kinetics on the particle size, the start time of the continuously added stream and the feed rates were adjusted for each seed type and level to ensure similar instantaneous conversions during the course of the process. From the figure it can be seen that the 0.0280 μm diameter seed maintains seed control from 0.2500 up to 0.4500 μm. This range of seed control was extended to 0.5800 μm with the 0.0650 μm seed and to 0.7500 μm with the 0.1750 μm seed. The 1.0 μm particle was obtained with a seed having a diameter of 0.3200 μm.

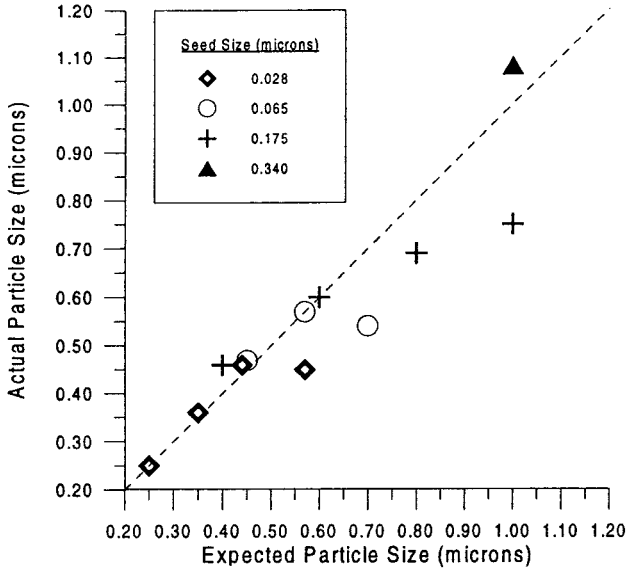

Figure 14. Actual versus calculated particle size of latexes made with seeds of various sizes.

Table 6. Apparent Molecular Weight of Latex Seeds

seed size (μm)	M_n	M_w
0.028	18 700	61 200
0.065	46 400	236 000
0.175[a]	26 000	134 000
0.320	8 100	52 400

[a] Insoluble gel present.

As seen in the Table 6, the seeds in the above study varied not only in size but also in molecular weight. The reason for this is that the large seeds needed to successfully make the large hollow particles were a significant weight fraction of the initial stage polymer. Since low molecular weight initial stage polymer is needed to ensure encapsulation of the hydrocarbon, adjustments to seed molecular weight and composition were examined to ensure adequate swelling and encapsulation of the hydrocarbon mixture early in the process. For example, making the 1 μm particle with a 50% void fraction of hydrocarbon with a seed of 0.32 μm, the seed polymer weight introduced into the initial charge will be approximately 7% of the final particle weight. This seed concentration amounts to a significant percentage of the polymer in the initial charge during the encapsulation stage. For example, in all the data present so far in this paper, 30% of the monomer to be polymerized was in the initial charge, with 70% continuously added during the stabilization stage. With the instantaneous conversion level of approximately 33%, cited previously as necessary to establish a surface locus, the seed would constitute approximately 40% of the polymer in the initial charge at the start time of the continuously added

Table 7. χ Values in the Simulations

interaction	χ value
nonsolvent−solvent	0.5
solvent−polymer	0.43
nonsolvent−polymer	1.0

monomer charge. To ensure encapsulation and morphological control with large particles with large void fractions, the molecular weight of the seed, the instantaneous conversion at the point at which the second monomer charge was introduced, and the ratio of monomer in the initial charge and continuously added stream were examined. Low molecular weight seed proved affective in making a large hollow particle with this process with a 50% void fraction.

Equilibrium Model. In dealing with the thermodynamics of encapsulation in an emulsion polymerization, there has been a significant development of ideas in the literature. Thermodynamic control of particle morphology has been described predominantly in terms of the interfacial energies between the components.[29,30] The simplest model experimentally examining the role of surface tension was described by Torza and Mason with their study of two immiscible hydrocarbons in water.[31] This concept was later expanded to polymer/hydrocarbon particles[32,33] and multipolymer particles.[34] The preferred morphology in these theories is defined as that which has the lowest interfacial free energy. However, the situation is complicated by the fact that thermodynamic equilibrium is assumed. This can be achieved with model hydrocarbon systems but may not be applicable during a polymerization. Furthermore, components typically in an emulsion polymerization, such as initiator type and level, monomer types, and surfactant, all influence the final morphology.[35,36] Independent of the physical assumption, sufficient data are frequently not available for applying a theory, e.g., interfacial energies between the components.

We have modeled the complex equilibria between the three distinct phases present in this process. These phases were defined in Figure 9 and included the free droplets of the hydrocarbon mixture (phase I), the polymer-rich phase within the particle (phase II), and the nonsolvent phase within the particle (phase III). Utilizing the Flory−Huggins equation for the free energy of mixing and the Gibbs−Thomas equation for the interfacial free energy,[37] a set of three equilibrium equations was constructed, one for each component. This involved defining the interaction parameters, χ values, and an assumption of the polymer molecular weight, which in this case was 10 000. The former were defined from the literature as well as experiment. Table 7 shows the values used in the simulation. Calculation of the corresponding equilibrium compositions involved solving these simultaneous equations. This was performed using the MINPACK subroutine HYBRD which utilizes a modified Powell hybrid method.[38]

Figure 15 is a ternary diagram for the calculated equilibrium within the growing polymer particle which designates the single-phase and two-phase regions. It identifies the compositions of phase II and phase III as well as the interfacial tension between phase I and II for the equilibrium condition between all three phases. Included in the figure is the compositional path the encapsulation process takes during the initial stage (Table 2). The desired phenomenon for encapsulation is for phase II and phase III to be stable relative to

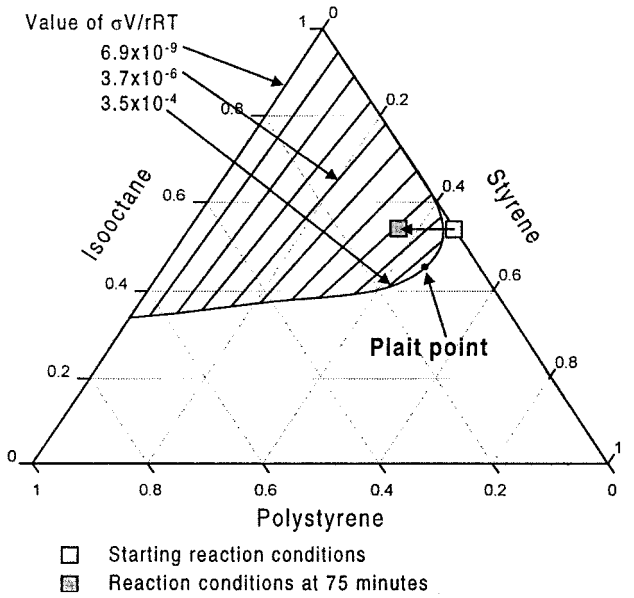

Figure 15. Equilibrium ternary diagram of phases within the particle (MW = 10 000).

phase I. This will occur if the overall system composition is within the two-phase region and if the surface tension term is less than that which defines an equilibrium between all three phases. Included in the diagram are values for the interfacial free energy term ($\sigma V/rRT$) of the organic droplets used in the model.

There are several significant details in this diagram. First, at a high interfacial free energy, the dispersion of the mixed hydrocarbon will not be stable. Only relatively large suspension-size reservoirs of the hydrocarbon mixture are present dispersed by the agitation in the reactor. Under these conditions encapsulation becomes problematic. Without a well-dispersed hydrocarbon mixture, styrene monomer dominates the migration from the organic mixture to the nucleation sites, as in a traditional emulsion polymerization. This leads to single-phase polymer particles. Second, the instantaneous composition of the batch is critical to producing the desired structure. Too low of an instantaneous monomer conversion results in a styrene-rich hydrocarbon phase, which can solubilize the polymer. Compositionally, it is best to keep the system near the plait point; i.e., the homogeneous phase is on the verge of becoming two phases. This allows for the largest possible interfacial free energy while still providing for phase III to be stable relative to phase I.

Once the swollen polymer is formed on the surface of the hydrocarbon mixture, it will act as a monomer sink and a locus for adsorption of radicals from the continuous phase as in any emulsion polymerization. This is true provided the instantaneous compositions remains such that the polymer layer does not become solubilized by the hydrocarbon mixture, phase III. Cross-linking and increasing the molecular weight of the polymer layer ensures that as more styrene is introduced the phase-separated polymer is not excessively swollen or dispersed throughout phase III.

This simulation was expanded to consider the influence of high molecular weight polymer on these phase equilibria. The experimental data indicated that encapsulation was minimized if such a polymer was made initially. Since solubility is inversely proportional to the molecular weight, phase III will have a zero polymer

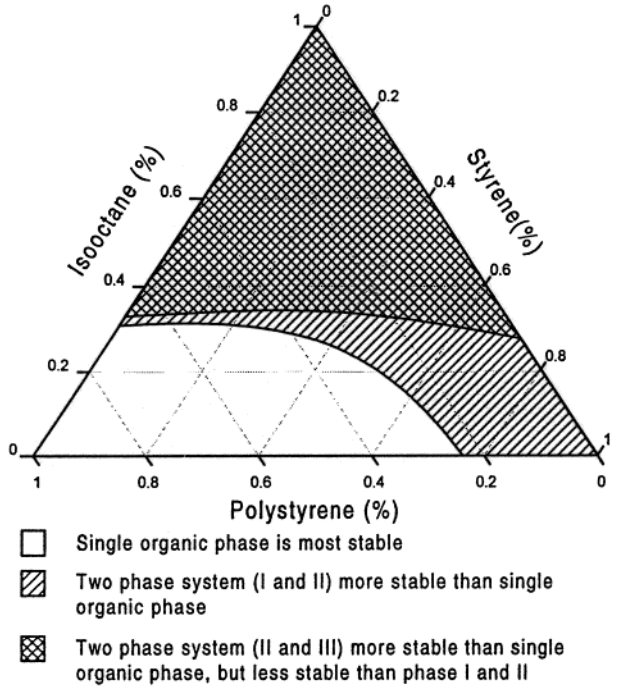

Figure 16. Equilibrium ternary diagram of phases within the particle (MW = infinity).

concentration under these conditions. Further if surface tension is ignored, there would be no thermodynamic difference between phase I and III. Both could therefore coexist at any ratio. If surface tension effects are present, phase III becomes unstable relative to phase I. Figure 16 shows the superimposed ternary diagrams derived from the model for the phase I/II equilibrium and phase II/III at infinite molecular weight. Superimposing the ternary diagrams shows the regions where multiphase systems are preferred. In the region without lines, a single organic phase is most stable, that is, a region of low isooctane and a significant styrene monomer/polymer concentration. In the region of parallel lines, a two-phase system consisting of phases I and II is more stable than a single organic phase characterized in the diagram. The crosshatched region represents where the two-phase system, phases II and III, is more stable than a single phase but less stable than the two-phase system, phases I and II. This model adequately describes the experimental finding that encapsulation with high molecular polymer is problematic, ultimately producing a polymer latex (phase II) and a separate nonsolvent layer (phase I).

This equilibrium modeling, however, oversimplifies this encapsulation system in a number of ways. The two ternary diagrams actually represent the initial and final states of this process. The nature of the transition between the two states is not addressed. It is apparent that the low molecular weight polymer formed initially has to become sufficiently stable as a shell that it behaves as a barrier to inversion. The inverted system is predicted by the model to be the most stable during formation of the high molecular weight (cross-linked) polymer matrix. Understanding the optimal instanteous conversion and kinetic conditions that facilitated full encapsulation had to be addressed empirically as described previously.

Another simplification involves ignoring mass transport limitations. To maintain equilibrium, it is obvious that the mass transport between the phases must be relatively fast as compared to the polymerization kinetics. The alcohol is expected to help in this regard, facilitating the transport of monomer, hydrocarbon, and oligomeric radicals from the droplets and serum phase of the emulsion to and between particles.

There are also a number of mathematical limitations in this equilibrium model which eliminate the possibility of utilizing them quantitatively. For simplicity, the polymer molecular weight is assumed to be monodispersed. In addition, the χ parameters were assumed to be independent of concentration and temperature. Further, the effects of initiator, acid comonomers, and alcohol are ignored.

Conclusions

It is possible to encapsulate within an emulsion polymerization a nonsolvent hydrocarbon for the polymer. A two-stage process enables formation of latex particles with voids. Particle morphology can be adjusted over a wide latitude from hollow or diffuse microvoids. The two stages of the process are distinguished by the molecular weight of the polymer being formed. Initially a low molecular weight polymer is synthesized in a batch charge containing both the monomer and hydrocarbon. As monomer is consumed, the polymer phase separates predominately near the surface of the dispersed mixture. Subsequently, this shell polymer serves as a locus for the development of a cross-linked network. Kinetic and thermodynamic variables are crucial to the control of morphology and the extent of encapsulation. These include the level of conversion of the initial batch charge of monomer prior to formation of the network, an amount of water-miscible alcohol present in the continuous phase, and the instantaneous level of conversion during the formation of the network. An equilibrium model was developed on the basis of the Flory−Huggins theory that was successful in characterizing the initial and final stages of this process.

Acknowledgment. This emulsion encapsulation process was first developed in 1985 and worked on intermittently during the intervening years. During this period, many people contributed to the experimental work and provided insights into this technology. The authors acknowledge the many contributions of their colleagues over the years, with special thanks to William E. Cohrs, Yohannes Chonde, Kostas S. Avramidis, Karen L. Wallace, Mary Chen, Clark J. Cummings, Chris Papouras, and Michael Cloeter. The evolution of this technology was also highly dependent on the microscopy data provided by Joan Marshall of Dow's Analytical Sciences Lab, for which the authors are grateful.

Supporting Information Available: Derivation of the equilibrium equations and ternary diagrams for the various phases of the system. This material is available free of charge via the Internet at http://pubs.acs.org.

References and Notes

(1) Strauss, J. *Surf. Coat. Aust.* **1987** *24*, 6.
(2) Dowling, D.; Grange, B. Lestarquit, Congr. FATIPEC 1986 Vol 1/A 117-44.
(3) Kaji, T.; Kami, Pa *Gikyoshi* **1992**, *46*, 271.
(4) Brown, J. T. *TAPPI Proceedings*, 1991 Coating Conference, p 113.
(5) Kowalski, A.; Vogel, M.; Blankenship, R. M. US Patent 4,-427,836, 1984.

(6) Kowalski, A.; Blankenship, R. M. US Patent 4,468,498, 1984.
(7) Kowalski, A.; Vogel, M. US Patent Number 4,469,825, 1984.
(8) Blankenship, R. M.; Kowalski, A. US Patent 4,594,363, 1986.
(9) Kowalski, A.; Vogel, M. US Patent 4,880,842, 1989.
(10) Blankenship, R. M. US Patent 5,494,971, 1996.
(11) Nippon Zeon KK, Japanese Patent 052779409 A, 1993.
(12) Kaino, M.; Takagishi, Y.; Toda, H. US Patent 5,360,827, 1994.
(13) Mitsui Toatsu Chem Inc., Japanese Patents 06073139 and 06073138A, 1994.
(14) Nippon Zeon KK, Japanese Patent 07021011, 1995.
(15) McDonald, C.; Chonde, Y.; Cohrs, W.; MacWilliams, D. US Patent 4,973,670, 1990.
(16) Small, H.; Saunders, F. L.; Langhorst, M. A. *Adv. Colloid Interface Sci.* **1976**, *6*, 237.
(17) McGowan, G. R.; Langhorst, M. A. *J. Colloid Interface Sci.* **1982**, *89*, 94.
(18) *N*,*N*-Diethylhydroxylamine, Aldrich Chemical Co., Milwaukee, WI.
(19) Odian, G. *Principles of Polymerization*, 2nd ed.; John Wiley & Sons: New York; 1981; p 329.
(20) *Polymer Handbook*, 3rd ed.; Brandrup, J., Immergut, E., Eds.; John Wiley & Sons: New York; 1989; Chapter II, p 94.
(21) Ball, D. L.; Crutchfield, M. M.; Edwards, J. O. *Macromolecules* **1969**, *25*, 1599.
(22) McIsaac, J. E., Jr.; Edwards, J. O. *Macromolecules* **1969**, *34*, 2565.
(23) Bida, G.; Ruggero, C.; Edwards, J. O. *Int. J. Chem. Kinet.* **1973**, *5*, 859.
(24) Gilbert, R. G. *Emulsion Polymerization: A Mechanistic Approach*; Academic Press: New York, 1995; pp 67−70.
(25) *Handbook of Physic and Chemistry*, 53rd ed.; Weast, R. C., Ed.; CRC Press: Cleveland, OH, 1972; p F-29.
(26) Odian, G. *Principles of Polymerization*, 2nd ed.; John Wiley & Sons: New York, 1981; p 271.
(27) *Emulsion Polymerization and Emulsion Polymers*; Lovell, P. A., El-Aasser, M. S., Eds.; John Wiley & Sons: New York, 1997; Chapter 2.
(28) Croucher, M. D.; Winnik, R. A. In *Scientific Methods for the Study of Polymer Colloids and Their Applications*; Candau, F., Ottewill, R. H., Eds.; NATO ASI Series; Kluwer Academic: Boston, 1990; Vol. 303, pp 35−72.
(29) Durand, Y. G.; Sundberg, D. C. In *Technology for Waterborne Coatings*; Glass, J. E., Ed.; ACS Symposium Series 663; American Chemical Society: Washington, DC, 1997; Chapter 3.
(30) Dimonie, V. L.; Daniels, E. S.; Shaffer, O. L.; El-Aasser, M. S. In *Emulsion Polymerization and Emulsion Polymers*; Lovell, P. A., El-Aasser, M. S., Eds.; John Wiley & Sons: New York; 1997; Chapter 9.
(31) Torza, S.; Mason, S. *J. Colloid Interface Sci.* **1970**, *33*, 67.
(32) Berg, J.; Sundberg, D. C.; Kronberg, B. *Microencapsulation* **1989**, *6*, 327.
(33) Sundberg, D. C.; Cassasa, A. J.; Pantazopoulos, M. R.; Muscata, B.; Kronberg, B.; Berg, J. *J. Appl. Polym. Sci.* **1990**, *41*, 1425.
(34) Lee, S.; Rudin, A. In *Polymer Latexes: Preparation, Characterization, and Applications*; ACS Symposium Series 492; American Chemical Society: Washington, DC, 1992; Chapter 15.
(35) Cho, I.; Lee, K.-W. *J. Appl. Polym. Sci.* **1985**, *30*, 1903.
(36) Daniel, J. C. *Makromol. Chem., Suppl.* **1985**, *10/11*, 403.
(37) Poehlein, G. In *Encyclopedia of Polymer Science and Engineering*; Mark, H. F., Bikales, N. M., Overberger, C. G., Menges, G., Eds.; John Wiley & Sons: New York, 1986; Vol. 6, pp 30−33.
(38) Garbow, B. S.; Hillstrom, K. E.; Jorge, J. M. MINPAC Software, Argonne National Laboratory, 1980.

MA991284E